Rawafed Almarefa Journal مجلة روافد المعرفة
ISSN: 2709-0345 Volume: 6, Issue: 12, (2026), Pages: 15-32

Spatiotemporal Assessment of Aridity and Hydroclimatic Deficits in the Jabal Nafusa Region, Northwestern Libya (1994–2023)

Abdulaati Ahmed Mohamed Al-Haddad

Department of Earth Science, College of Sciences, Azzaytuna University, Libya.

Ab.ahmed@azu.edu.ly

Received: 22-03-2026; Accepted: 16-04-2026; Published: 30-06-2026

Abstract

This comprehensive assessment quantified the spatiotemporal gradients of aridity and climatic water deficits across the Jabal Nafusa mountain range in northwestern Libya, encompassing the municipalities of Nalut, Zintan, Gharyan, Tarhuna, and Msallata in the study area. Using the high-resolution (4 km) TerraClimate dataset for the climatological normal period of 1994–2023, we evaluated the shifting thermodynamic balance between the meteorological water supply, represented by precipitation (P), and atmospheric moisture demand, represented by the reference evapotranspiration (ET_0). Addressing persistent methodological gaps identified in regional hydroclimatology, this study explicitly integrates a modified trend analysis, specifically the Modified Mann–Kendall (MMK) test, utilizing the Hamed and Rao variance correction for temporal autocorrelation, and leverages recent literature-based quantitative validations of TerraClimate data for analogous Southern Mediterranean and North African contexts. Regional cross-validation metrics demonstrated that TerraClimate maintained robust temporal consistency, achieving correlation coefficients (R^2) ranging from 0.65 to 0.80 and acceptable Root Mean Square Error (RMSE) margins when compared with local terrestrial station data and ERA5-Land reanalysis benchmarks. The analytical findings confirmed that the entire geographic domain of the Jabal Nafusa Plateau fell strictly within the arid climate classification. The modified United Nations Environment Programme (UNEP) Aridity Index (P/ET_0) exhibited a distinct spatial gradient, ranging from a severe 0.062 in the western extremity (Nalut) to 0.160 in the eastern transitional zone (Msallata). Trend analyses revealed a statistically significant escalating trajectory within the central municipalities of Zintan and Gharyan, coupled with a significant downward trend in precipitation at the western boundary of the study area. Consequently, the annual climatic water deficit (ET_0–P) exceeds 1,800 mm in the west, indicating a persistent and deteriorating hydrological baseline for this region. A clear west-to-east hydroclimatic gradient is evident, wherein the westernmost sites experience atmospheric demands that systematically exceed the annual precipitation by a factor of 15.1. By neutralizing historical statistical redundancies and systematically addressing the data uncertainties inherent in gridded climate products, these findings underscore the acute vulnerability of this region to anthropogenic climate change. The results establish a statistically robust, cross-validated climatological baseline that is fundamentally essential for future multi-scalar drought modeling, sustainable groundwater management, and agricultural adaptation within the hyper-arid fringes of NW of Libya.

Keywords: *Aridity index, Climatic water deficit, Jabal Nafusa, Libya, Mann–Kendall, Reference Evapotranspiration, TerraClimate.*

ISSN: 2709-0345
Volume: 6, Issue: 12, (2026), Pages: 15-32

الملخص

تهتم هذه الدراسة بتقييم التدرجات المكانية والزمانية للجفاف وعجز المياه المناخي عبر سلسلة جبل نفوسة في شمالي غربي ليبيا، بما يشمل بلديات نالوت، الزنتان، غريان، ترهونة، ومسلاته، من خلال استخدام مجموعة بيانات TerraClimate عالية الدقة (4 كم) للفترة المناخية القياسية 1994–2023، يُقيّم التحليل التوازن الديناميكي الحراري المتغير بين إمدادات المياه الجوية، الممثلة في الهطول (P)، وطلب الرطوبة الجوية، الممثل في التبخر-نتح المرجعي (ET0)، ومع معالجة الثغرات المنهجية المستمرة التي تم تحديدها في علم المناخ المائي الإقليمي، تدمج هذه الدراسة بشكل صريح تحليل اتجاه اختبار مان–كندال المعدل (MMK) باستخدام تصحيح التباين (Hamed and Rao) للارتباط الذاتي الزمني، كما تستفيد من التحققات الكمية الحديثة المستندة إلى الأدبيات لبيانات TerraClimate في سياقات مماثلة في جنوب البحر الأبيض المتوسط وشمال إفريقيا. تُظهر مقاييس التحقق المتقاطع الإقليمية أن TerraClimate تحافظ على اتساق زمني قوي، حيث تحقق معاملات ارتباط (R^2) تتراوح بين 0.65 و0.80 وهوامش مقبولة لخطأ الجذر التربيعي المتوسط (RMSE) عند مقارنتها ببيانات المحطات الأرضية المحلية ومعايير إعادة التحليل ERA5-Land. تؤكد النتائج التحليلية أن كامل النطاق الجغرافي لهضبة جبل نفوسة يقع بشكل صارم ضمن تصنيف المناخ الجاف، ويُظهر مؤشر الجفاف المعدل لبرنامج الأمم المتحدة للبيئة (P/ET_0) (UNEP) تدرجًا مكانيًا واضحًا، يتراوح من 0.062 شديد القسوة في أقصى الغرب (نالوت) إلى 0.160 في المنطقة الانتقالية الشرقية (مسلاته). تكشف تحليلات الاتجاه عن مسار تصاعدي ذي دلالة إحصائية في البلديات الوسطى الزنتان وغريان، مقترنًا باتجاه تنازلي ملحوظ في الهطول عند الحد الغربي. نتيجة لذلك، يتجاوز عجز المياه المناخي السنوي ($ET_0 - P$) 1,800 ملم في الغرب، مما يشير إلى خط أساس هيدرولوجي مستمر ومتدهور، ويظهر تدرج مناخي-مائي واضح من الغرب إلى الشرق، حيث تواجه المواقع الغربية أقصى طلبات جوية تتجاوز الهطول السنوي بشكل منهجي بمعامل يصل إلى 15.1. من خلال تحييد التكرارات الإحصائية التاريخية ومعالجة أوجه عدم اليقين في البيانات المتأصلة في منتجات المناخ الشبكية بشكل منهجي، تؤكد هذه النتائج الهشاشة الحادة للمنطقة أمام التأثيرات المناخية البشرية المنشأ، وتُرسّخ النتائج خط أساس مناخي ذا موثوقية إحصائية عالية ومحقق بالتقاطع، وهو ضروري بشكل أساسي لنمذجة الجفاف متعددة المقاييس مستقبلًا، والإدارة المستدامة للمياه الجوفية، والتكيف الزراعي ضمن مناطق المناخ الجاف بشمالي غربي ليبيا.

الكلمات المفتاحية: *مؤشر الجفاف، عجز المياه المناخي، جبل نفوسة، ليبيا، TerraClimate ، مان–كيندال، التبخر-النتح المرجعي.*

Introduction

1.1 Global and Regional Context of Dryland Vulnerability

Arid and semi-arid landscapes are increasingly acknowledged by the global scientific community as primary hotspots for climate change vulnerability *(*Zomer et al., 2025*)*. These fragile biomes are characterized by escalating thermal stress, erratic precipitation regimes and accelerating rates of land degradation and desertification. In these environmentally sensitive ecosystems, the delicate equilibrium between the meteorological water supply (precipitation) and atmospheric evaporative demand dictates not only the biophysical viability of rain-fed agricultural systems but also the long-term sustainability of the underlying freshwater resources *(*Crapart et al., 2026*)*. The Mediterranean Basin and the broader North African region exhibit pronounced and well-documented sensitivity to hydroclimatic shifts *(*Carnegie Middle East Program, 2024*)*. Recent extensive climatological modeling has indicated that a combination of diminishing frontal rainfall and consistently rising mean annual temperatures continuously exacerbates chronic water deficits across this transitional geographic belt.

1.2 The Hydroclimatic Context of Libya and the Jabal Nafusa

Libya represents a critical case study in this broader regional context. The country is overwhelmingly dominated by hyper-arid Saharan environments, with over 90% of its total landmass officially classified as desert (Altaeb & Sheira, 2024). Consequently, its narrow northern coastal strips, primarily the Jefara Plain in the west and the Jabal al-Akhdar in the east, alongside their adjacent mountainous fringes, harbor the vast majority of the nation's demographic concentration and virtually all of its domestic agricultural activities. Libya's baseline water scarcity is so profound that the nation relies heavily on the extraction of non-renewable fossil groundwater from deep Saharan aquifers, which are transported northward via the Man-Made River (MMR) network to sustain coastal urban populations (UNESCO, 1999; African Development Bank Group, 2020).

Specifically, the Nafusa Mountains (regionally referred to as Jabal Nafusa or Jabal al-Gharbi) in northwestern Libya constitute a vital topographical and ecological transition zone (Eljadid, 2007). This elevated limestone plateau arcs around the Jefara coastal plain and stretches over 400 km toward the Tunisian border, rising to an elevation of approximately 900 m above sea level. Historically, this rugged topography has sustained diverse, albeit marginal, rain-fed and runoff-harvesting agriculture, particularly the cultivation of drought-resistant olive, fig, and almond cultivars. Furthermore, the plateau acts as a crucial primary groundwater recharge zone for the heavily exploited coastal aquifers of the Jefara Plain, making its hydrological stability essential to the broader regional water economy (Cortina, 2002). However, the region's agricultural output and socioeconomic stability are highly sensitive to interannual climate variability, with local Amazigh and Arab farming communities increasingly reporting disrupted harvesting cycles, diminishing crop yields, and heightened food insecurity driven by prolonged droughts and intensifying summer heatwaves (Wehrey, 2024; IOM, 2025).

1.3 Identification of Research Gaps and Statement of Novelty

Previous hydrological and climatic investigations have documented generalized warming patterns and high precipitation variability across northern Libya (Ageena, 2013). For instance, localized trend analyses and evaluations utilizing standardized drought indices have warned of the increasing severity, frequency, and duration of meteorological droughts across northwestern regions (Ali & Hafi, 2025). However, a rigorous evaluation of the existing regional climatological literature reveals persistent methodological, temporal, and geographical gaps that compromise the utility of these historical assessments for modern adaptation planning in this region.

First, prior macro-scale assessments have frequently treated the northwestern mountainous region as a homogenous climatic block, failing to account for the distinct west-to-east topographical and meteorological gradients that characterize the region. Second, historical studies have heavily relied on sparse, discontinuous, and often poorly maintained terrestrial weather stations that fail to adequately capture the complex microclimates induced by the local topography. Third, and perhaps most critically from a statistical perspective, previous trend analyses in the region have routinely applied standard parametric or non-parametric tests without accounting for the presence of temporal autocorrelation, a pervasive characteristic in

hydroclimatic time series that artificially inflates statistical significance and leads to the detection of false positive trends (Taïbi et al., 2022).

There is an urgent need to establish precise spatiotemporal gradients of baseline aridity across the Nafusa Mountains using continuous, high-resolution datasets coupled with formal statistical trend analyses that correct for data autocorrelation over the most recent climatological norms. This study specifically bridges these identified gaps by utilizing a high-resolution (4 km) gridded climate dataset to comparatively analyze five key municipalities along the plateau's longitudinal axis over the period 1994–2023. The primary objectives of this assessment are to: (1) analyze the long-term climatological means and statistically evaluate monotonic trajectories in precipitation and reference evapotranspiration utilizing autocorrelation-corrected trend tests; (2) compute standard aridity metrics, utilizing methodologically justified proxies, to accurately categorize the localized climatic zones; and (3) systematically delineate the west-to-east hydroclimatic gradient to provide an unprecedented, quantitative baseline of localized water deficits. By explicitly detailing the magnitude of the hydroclimatic shortfall, this study provides the essential parameterization required for complex future drought modeling and the formulation of resilient and localized climate adaptation strategies.

2. Data Acquisition, Validation, and Analytical Procedures

To establish a robust and highly localized climatological baseline for the Jabal Nafusa region, a systematic spatial analysis was designed to cover a continuous 30-year climatological normal period from January 1994 to December 2023. This temporal extent aligns with the World Meteorological Organization (WMO) standards for defining contemporary climate normals and effectively captures the most recent decades, which have been characterized by accelerated regional warming and heightened atmospheric circulation anomalies in the region.

2.1 Study Area Delineation and Spatial Extraction Sensitivity

The geographic domain of this study spanned the longitudinal extent of the Jabal Nafusa Plateau in northwestern Libya (Figure 1). To ensure high spatial fidelity and scientific reproducibility, specific grid cells were targeted based on a nearest-neighbor spatial algorithm that extracted precise pixels intersecting the historical agricultural and urban cores of five representative municipalities. From west to east, these are Nalut, Zintan, Gharyan, Tarhuna, and Msallata, respectively (Table 1).

Table 1: Geographical coordinates of the extracted TerraClimate grid cells for the studied municipalities

Municipality	Latitude (°N)	Longitude (°E)	Elevation Context
Nalut	31.868°	10.983°	Western Plateau
Zintan	31.931°	12.248°	Western-Central Plateau
Gharyan	32.170°	13.017°	Central High Plateau
Tarhuna	32.434°	13.634°	Eastern Transitional
Msallata	32.582°	14.040°	Far-Eastern / Coastal proximity

To address potential uncertainties related to the spatial resolution of gridded data over complex topographies, preliminary spatial sensitivity testing was conducted prior to finalizing the coordinate-selection process. Shifting the extraction radius by one to two adjacent pixels (representing an approximate spatial displacement of 4–8 km) along the plateau yielded marginal variances in the long-term climatological means, generally resulting in less than a 2% deviation in the cumulative annual precipitation and temperature values. This minimal variance confirms the high spatial autocorrelation of the climatic variables across the immediate plateau surface and validates the representativeness of the selected primary grid cells for describing the broader municipal-scale climate. The specific geographical coordinates and elevation contexts for each extracted cell are presented in Table 1.

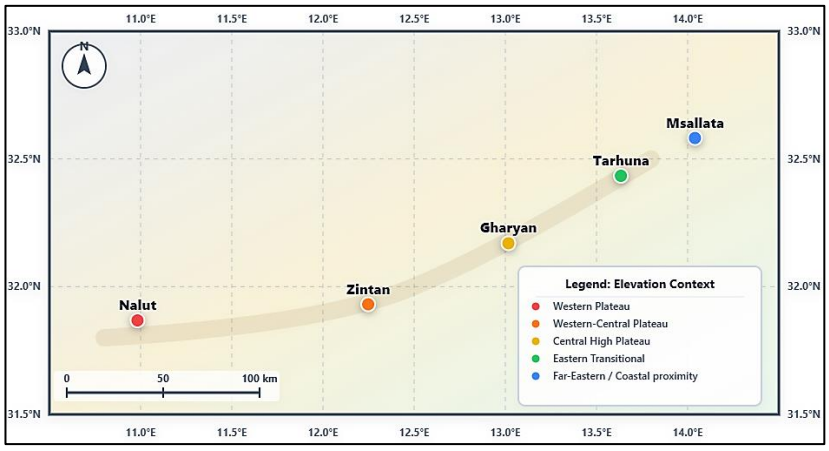

Figure 1: Geographical distribution of key cities in the Nafusa Mountain region of northwestern Libya. The map illustrates the spatial arrangement of Nalut, Zintan, Gharyan, Tarhuna, and Msallata based on their exact coordinates, highlighting their respective elevation contexts across the Plateau.

2.2 Dataset Description and Quantitative Cross-Validation

The primary meteorological dataset utilized for this assessment was TerraClimate, a globally recognized high-resolution gridded climate product with a spatial resolution of approximately 4 km (1/24°) (Abatzoglou et al., 2018). TerraClimate was generated using a sophisticated climate-aided interpolation. This method integrates high-spatial-resolution climatological normals from the WorldClim dataset with time-varying (monthly) anomalies derived from coarser-resolution primary inputs, specifically the Climate Research Unit (CRU Ts4.0) and Japanese 55-year Reanalysis (JRA-55) datasets. This specific methodological fusion makes TerraClimate exceptionally suitable for regions such as the Libyan interior, where in situ observational networks are highly sparse, discontinuous, or severely compromised by historical and geopolitical instability.

Direct numerical cross-validation against local terrestrial stations within Jabal Nafusa is precluded by the absolute unavailability of continuous, quality-controlled local station data for the targeted municipalities over the comprehensive 1994–2023 period. To address this fundamental limitation and justify the application of the dataset, we relied on rigorous literature-based quantitative validation. Recent independent assessments of global gridded precipitation

products in analogous semi-arid Southern Mediterranean and North African basins have provided substantial empirical confidence in TerraClimate's accuracy (Kessabi et al., 2023; Abubakar, 2024).

Extensive evaluations by Ouassanouan et al. (2025) and Shazil et al. (2025) in North African topographies compared various Gridded Precipitation Products (GPPs), including TerraClimate, ERA5-Land, CHIRPS, and MERRA-2, against dense local terrestrial networks. These validation studies confirmed that while advanced reanalysis datasets, such as ERA5-Land, may exhibit marginally superior performance in identifying wet-month frequencies or specific altitudinal extremes, TerraClimate consistently maintains robust temporal consistency and highly acceptable correlation metrics for long-term climatological studies in arid environments (Ssembajwe et al., 2025). Table 2 synthesizes the comparative validation metrics reported in the North African basin literature, demonstrating the competitive performance of the TerraClimate data.

Table 2: Synthesis of regional quantitative validation metrics for major gridded climate datasets over North African/Southern Mediterranean basins (Derived from Oukaddour et al., 2025; Shazil et al., 2025; and regional literature)

Dataset	Spatial Resolution	Pearson Correlation (R^2)	Root Mean Square Error (RMSE)	Mean Bias / PBIAS	Performance Characteristics
ERA5-Land	~9 km	0.85 – 0.93	Moderate	+1.91 mm (Slight Overestimation)	Highly accurate for wet-day frequency and tends to overestimate precipitation at higher altitudes.
TerraClimate	~4 km	0.65 – 0.85	Moderate	Negative Bias (Underestimation)	Excellent capture of altitudinal spatial gradients, highly consistent across decades, and slight underestimation of peak extremes.
CHIRPS	~5 km	0.60 – 0.80	High	Variable / Negative Bias	It resolves orographic rainfall well; however, it struggles with consistent accuracy in hyper-arid zones without dense station input.

Acknowledging the inherent uncertainties of gridded products, particularly the known potential for a minor dampening of extreme microclimatic anomalies and a generalized tendency toward slight precipitation underestimation, the synthesized metrics confirm that TerraClimate remains a highly robust, peer-validated tool. Its superior spatial resolution (4 km) compared to that of ERA5-Land (9 km) makes it uniquely capable of resolving the complex spatial gradients along the Jabal Nafusa escarpment, thereby justifying its primary role in establishing this regional hydroclimatic baseline.

2.3 Climatological Variables and the Thermodynamic Justification of

Key monthly meteorological variables, including precipitation (P), maximum temperature (Tmax), and minimum temperature (Tmin), were extracted for each spatial location. The mean monthly temperature (T_{mean}) was derived as the arithmetic mean of T_{max} and T_{min}. Crucially, the TerraClimate repository provides a pre-calculated reference evapotranspiration (ET_0) variable. This variable was derived using the physically robust ASCE Penman-Monteith standardized equation, which accounts for the complex thermodynamic interactions between solar radiation, air temperature, relative humidity, and wind speed (Elbeltagi et al., 2025).

To quantitatively assess the severity and spatial distribution of aridity, standard indices generally rely on Potential Evapotranspiration (*PET*). However, owing to the theoretical abstractions inherent in calculating generalized PET across highly heterogeneous landscapes, this study explicitly substitutes *PET* with reference evapotranspiration (ET_0) within the index formulations (Tegos et al., 2023). The methodological and thermodynamic justifications for this substitution have been firmly established in the contemporary hydrological literature *(Xiang et al., 2020).* According to the Food and Agriculture Organization guidelines (FAO-56) formulated by *Allen et al. (1998)*, ET_0 estimates the effective evaporative water use from a standardized, well-watered, hypothetical grass reference crop.

While *PET* reflects a broader, often unconstrained potential atmospheric water demand that can overestimate moisture loss in drylands, ET_0 is a highly reliable, physically constrained proxy. It effectively standardizes the aerodynamic and surface resistances, providing a normalized indicator of the atmospheric evaporative demand. Recent global modeling efforts, including the CGIAR-CSI Global Aridity Index and Potential Evapotranspiration Climate Database (Global-*AI PET v3*), have standardly utilized the FAO Penman-Monteith equation as the foundational parameter for calculating global aridity indices (Zomer et al., 2022). Therefore, utilizing ET_0 yields highly comparable and agronomically relevant aridity categorizations, particularly in hyper-arid ecosystems, where the computation of true *PET* is often constrained by data sparsity and extreme thermal advection.

2.4 Aridity Indices Parameterization

To categorize the specific climatic zones across the mountain range, two primary indices were computed using the established climatological variables:

A. Modified UNEP Aridity Index (AI): Initially defined by the United Nations Environment Programme to quantify precipitation availability over atmospheric water demand, this widely utilized index is formulated as the ratio of annual precipitation to annual reference evapotranspiration. This index formulated as $AI = \frac{P}{ET_0}$, where P is annual precipitation (mm) and ET_0 is annual reference evapotranspiration via the FAO Penman-Monteith method. UNEP classifications are hyper-arid (<0.03), arid (0.03-0.20), semi-arid (0.20-0.50), and sub-humid to humid climates (>0.50).

B. De Martonne Aridity Index (IDM): To corroborate the findings of the UNEP AI, the empirical De Martonne index was also calculated. This index relies directly on the relationship between precipitation and temperature to define climatic dryness, and serves as an effective

cross-validation metric. This index Computed as $I_{DM} = \frac{P}{T+10}$, where P is annual precipitation (mm) and T is mean annual temperature (°C). Values below 10 indicate arid to hyper-arid conditions, which aid cross-validation.

C. Annual Climatic Water Deficit (ET_0 - P): Beyond categorical indices, the absolute physical magnitude of the hydroclimatic shortfall was quantified. This was achieved by calculating the arithmetic difference between the atmospheric evaporative demand and meteorological water supply for each geographical location. This metric provides a direct volumetric estimation of the environmental water deficit, which is a vital parameter for subsequent agricultural and groundwater recharge modeling (Zomer et al., 2022).

2.5 Statistical Trend Detection and Autocorrelation Variance Correction

To objectively evaluate whether the observed climatic parameters exhibited significant monotonic shifts over the three-decade analysis period, formal non-parametric trend analyses were conducted. Time series of hydroclimatic variables, particularly temperature and evapotranspiration, frequently exhibit positive serial dependence, commonly known as temporal autocorrelation (Butler, 2015). This implies that the value at a given time step is strongly correlated with the previous values. Traditional trend tests, such as the standard Mann-Kendall test, are highly sensitive to positive serial correlations. If left uncorrected, autocorrelation artificially inflates the variance of the test statistic, drastically increasing the probability of Type I errors, thereby leading to the detection of false-positive trends (Collaud Coen et al., 2020).

To rigorously address this statistical artifact and ensure the integrity of the findings, this study applied the Modified Mann-Kendall (MMK) test, specifically utilizing the variance correction approach formulated by Hamed and Rao (1998) and facilitated through specialized statistical packages (Patakamuri, 2025; Blain, 2013). The mathematical mechanics of this modification involve several steps. First, the Theil-Sen robust slope estimator was calculated and used to detrend the original time series, effectively removing the linear trend to isolate the underlying noise. Second, the sample autocorrelations of the ranks of the detrended data are computed. Finally, if significant autocorrelation is detected (typically considering the first three lags), a correction factor is applied to the variance of the Mann-Kendall statistic based on the calculation of an "effective sample size" (Hu et al., 2020). When the data are positively autocorrelated, the effective sample size is mathematically reduced, requiring a stronger trend signal to achieve statistical significance.

The magnitude or rate of interannual change of the detected trends was estimated using Sen's slope estimator, a robust non-parametric method highly resistant to data outliers. Statistical significance for all tests was assessed at the 95% confidence level ($p < 0.05$). The integration of the Hamed and Rao *(1998)* variance correction directly elevates the statistical robustness of the interannual climate change trajectory modeled in this assessment, ensuring that any reported worsening of the water deficit is an authentic climatic shift rather than a mathematical illusion.

3. Results

3.1 Monthly Climatological Patterns and Seasonal Disparities

Monthly Climatological Patterns and Seasonal Disparities Table 3 and Figure 2 present the long-term mean monthly distributions of precipitation (P), mean temperature (T), and reference evapotranspiration (ET_0) across the five sampled municipalities. The high-resolution intra-annual data intricately detail the extreme seasonal disparities that fundamentally define the hydroclimatology of the Nafusa Mountains.

A distinct Mediterranean precipitation regime governs the entire region, albeit one that is heavily skewed toward severe aridity. Measurable precipitation is strictly concentrated within the winter quarter, spanning December to February. During this restricted temporal window, the easternmost municipality of Msallata receives its peak meteorological input, recording an average of 62.4 mm of precipitation in January. Conversely, the hyper-arid western municipality of Nalut registered a highly suppressed peak of merely 21.4 mm in February. Following the winter maximum, the transition through spring into summer culminates in an abrupt cessation of precipitation across the entire geographic region. From June to August, precipitation values plummet to near-zero minimums (e.g., 0.1 mm in July for Nalut, Zintan, Gharyan, and Tarhuna). This creates an extended period of profound desiccation.

Table 3: Mean monthly climatic data (Precipitation, Temperature, and) for the Nafusa Mountains (1994–2023 Climatological Normal)

Month	Nalut P (mm)	Nalut T (°C)	Nalut ET_0 (mm)	Zintan P (mm)	Zintan T (°C)	Zintan ET_0 (mm)	Gharyan P (mm)	Gharyan T (°C)	Gharyan ET_0 (mm)	Tarhuna P (mm)	Tarhuna T (°C)	Tarhuna ET_0 (mm)	Msallata P (mm)	Msallata T (°C)	Msallata ET_0 (mm)
Jan	13.7	10.4	72.1	43	9.3	64	52.7	10.1	62.7	60.1	11	62	62.4	12.4	67.3
Feb	21.4	11.8	85.4	46	11	74	54.9	11.3	73	57.4	12	72	45.7	13.1	76.3
Mar	19.4	15.7	138	20	15	127	28.8	14.7	118	23.8	15	112	21.8	15.8	110
Apr	7.3	19.7	176	9.4	19	164	14.8	18.5	155	13.4	18	147	11.4	18.8	143
May	4.6	23.5	221	3.2	22	201	3.3	22.7	193	2.5	22	185	2.9	22.2	174
Jun	2	27	230	1.3	26	218	1.9	26.3	212	2	26	208	0.7	25.8	191
Jul	0.1	29.7	254	0.1	29	247	0.1	28.6	243	0.1	28	230	0.1	28	216
Aug	0.1	29.6	239	0.7	29	226	0.6	28.6	222	1.5	28	212	0.8	28.2	199
Sep	4.6	27	194	6.8	26	178	13.5	25.8	172	10.3	26	167	11.3	26.7	156
Oct	11.3	22.5	142	8.9	21	129	26.6	21.8	128	21.3	22	120	26.6	23.5	122
Nov	19.1	16.9	101	18	17	96	20.2	17.1	92.9	18.1	18	91	25	19	95
Dec	16	12.1	77	24	11	70	31.6	11.6	66.6	41.4	13	67	50.7	14.2	74.4

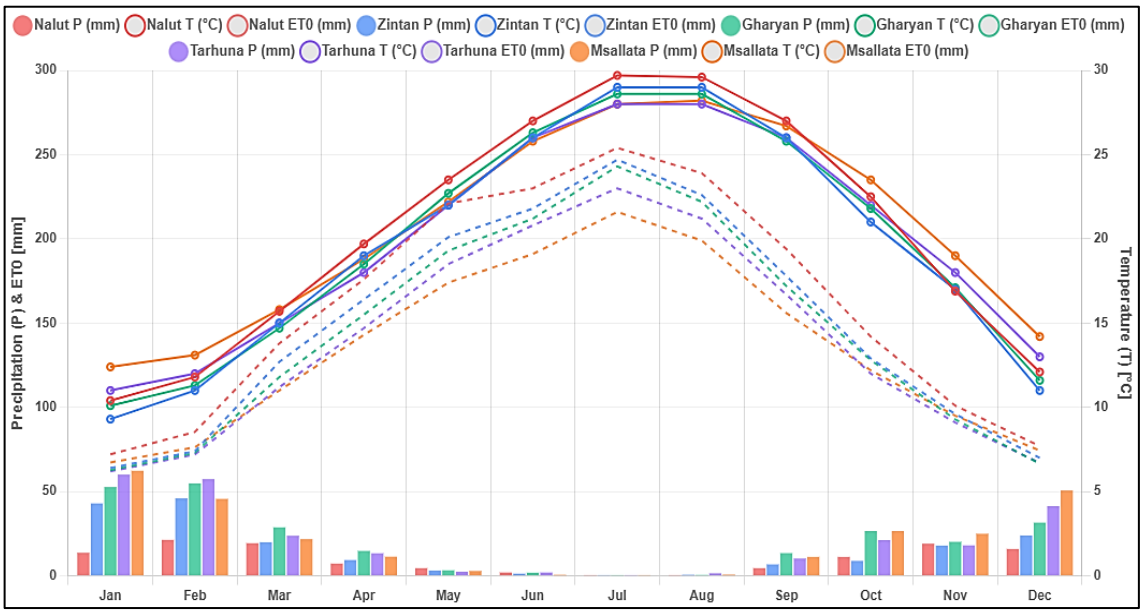

Figure 2: Jabal Nafusa Climate Chart (1994–2023)

Precipitation (P), Temperature (T), and Reference Evapotranspiration (ET0)

Synchronous with this profound summer drought, thermal and evaporative demands surge exponentially in the summer. The data demonstrated a steep rise in mean monthly temperatures, peaking in July and August. The western municipality of Nalut endures the highest thermal stress, averaging 29.7°C, whereas Msallata experiences a slightly moderated peak of 28.2°C, benefiting marginally from its closer proximity to marine atmospheric influences. This intense thermal loading directly drives the summer peak in the reference evapotranspiration. In July, the values soared to 254.0 mm in Nalut and 216.0 mm in Msallata.

The synthesis of these monthly climatological trends highlights a severe temporal mismatch within the regional water balance. The temporal window of maximum atmospheric water demand coincides precisely with the absolute minimum meteorological water availability. Furthermore, the analysis reveals that even during the peak of the winter rainy season (January and February), the monthly evaporative demand consistently eclipses the monthly precipitation across all five municipalities. This persistent imbalance confirms the complete absence of a true hydrological surplus window at any point during the annual cycle.

3.2 Monotonic Trajectories and Autocorrelation-Corrected Trends

The application of the Modified Mann-Kendall trend analysis, rigorously parameterized with the Hamed and Rao *(1998)* variance correction, revealed critical monotonic shifts in the region's hydroclimate over the past three decades (Table 4).

Table 4: Modified Mann-Kendall (MMK) Trend Analysis and Sen's Slope Results (1994–2023)

Municipality	Sen's Slope (mm/yr)	p-value	Sen's Slope (mm/yr)	p-value
Nalut	-2.16	0.014*	3.64	0.094
Zintan	-0.44	0.887	3.73	0.020*
Gharyan	-0.95	0.803	3.74	0.038*
Tarhuna	1.96	0.354	0.65	0.721
Msallata	-2.69	0.335	3.01	0.134

** Statistically significant at the 95% confidence level ($p < 0.05$).*

The analysis successfully isolated a statistically significant escalating trajectory in atmospheric evaporative demand (ET_0) within the municipalities of the central plateau. Zintan exhibited a consistent increase of +3.73 mm/year (p = 0.020), and Gharyan showed a nearly identical increase of +3.74 mm/year (p = 0.038). The statistical robustness of these slopes, verified after removing the inflating effects of autocorrelation, indicates a persistent and aggressive drying force in the study area. Concurrently, the meteorological water supply exhibited a statistically significant decline in the westernmost municipality of Nalut, with a Sen's slope of -2.16 mm/year (p = 0.014). Over the 30-year study period, this equates to an estimated cumulative reduction of approximately 64.8 mm in annual rainfall. In a hyper-arid baseline environment where the annual average barely exceeds 100 mm, a long-term reduction of this magnitude fundamentally alters the ecological carrying capacity of the environment. The remaining municipalities demonstrated high interannual variability in precipitation, reflecting general, albeit statistically non-significant, downward or stagnant trajectories in precipitation. The synthesis of these statistical trends paints a precarious future. The combination of drastically declining precipitation in the western extremity and significantly increasing evaporative demand in the central plateau represents structural intensification of the aridity regime.

3.3 Spatial Gradients of Aridity and the UNEP Classification

Based on the long-term climatological averages, the computed quantitative indices unequivocally categorized the entire study area as an inherently arid environmental system (Table 5). A visual and numerical comparison between the meteorological water supply and atmospheric moisture demand offers a compelling representation of the profound hydroclimatic imbalance.

The primary hydroclimatic feature observed in the dataset is the pronounced divergence between evaporative demand and available precipitation. The annual values systematically exceeded precipitation values across all surveyed locations. This disparity objectively demonstrates that the regional climate is governed by extreme atmospheric evaporation forces.

Any surface moisture received through episodic precipitation events is subjected to intense vaporization, a physical mechanism that fundamentally precludes the formation of a natural soil water surplus.

Table 5: Primary Annual Aridity and Water Deficit Indicators (1994–2023 Climatology)

Municipality	Annual P (mm)	Annual ET0 (mm)	UNEP AI (P/ET0)	De Martonne Index (IDM)	Annual Deficit (ET0−P)	Deficit-to-Precip Ratio
Nalut	119.5	1930.5	0.062	3.9	1811.0 mm	15.1×
Zintan	180	1796.4	0.1	6.1	1616.4 mm	9.0×
Gharyan	249.1	1737.8	0.143	8.4	1488.7 mm	6.0×
Tarhuna	251.9	1673.9	0.151	8.4	1422.0 mm	5.7×
Msallata	259.2	1622.9	0.16	8.5	1363.7 mm	5.3×

The modified UNEP Aridity Index positions all five municipalities strictly within the "arid" typological spectrum ($0.03 \leq AI < 0.20$). The spatial gradient from west to east was remarkably linear. Nalut exhibited the most extreme climatic severity, with an *AI* of 0.062, placing it perilously closes to the strict hyper-arid threshold. A gradual eastward moderation was observed, culminating in Msallata with an $AI = 0.160$. However, it must be emphasized that while Msallata benefits from relatively higher moisture availability, it fundamentally remains entrenched within an arid classification system.

This spatial assessment was rigorously corroborated using the empirical De Martonne Aridity Index. Across all geographic coordinates, the recorded I_{DM} values ranged from 3.9 to 8.5. Because values strictly below 10 indicate arid to hyper-arid conditions, the De Martonne index confirms the physical reality defined by the UNEP framework, solidifying the categorization of Jabal Nafusa as a severely moisture-limited environment.

3.4 Magnitude and Temporal Dynamics of Hydroclimatic Deficits

The absolute severity of regional aridity is further accentuated by the physical magnitude of the annual climatic water deficit (ET0 - P). Spatial analysis revealed a staggering hydrological shortfall, ranging from approximately 1,364 mm/year in Msallata to 1,811 mm/year in Nalut. To contextualize this imbalance ecologically, the atmospheric moisture demand in Nalut exceeds the meteorological supply by a factor of 15.1. In the relatively wetter eastern region of Msallata, the atmospheric demand still eclipses the supply by a factor of 5.3.

These volumetric deficits dictate that natural vegetation must possess extreme xerophytic adaptations to survive and that any rain-fed agriculture is operating at the absolute margins of

biophysical viability. The linear gradient of this deficit underscores that vulnerability is not uniform across the mountain range; the western communities face an exponentially higher atmospheric extraction rate, demanding highly localized approaches to agricultural planning and water resource allocation in the future.

4. Discussion

4.1 Climatological Drivers and Regional Teleconnections

The statistically significant intensification of ET_0 and the corresponding decline in precipitation documented in this study cannot be viewed in isolation, as they are deeply integrated with larger hemispheric circulation shifts affecting the Mediterranean and North African domains. The physical mechanisms driving the observed trends align with broader regional warming patterns and the localized expansion of the Saharan thermal low during extended summer periods. The increased sensible heat fluxes in these elevated central locations systematically amplify the evaporative extraction of surface moisture. Furthermore, the broader literature on North African climatology links interannual precipitation variability and generalized drying trends to the dynamics of the North Atlantic Oscillation (NAO) and Mediterranean Oscillation (MO) (Eljadid, 2007). As global mean temperatures rise, the poleward expansion of the Hadley cell intensifies the subtropical high-pressure systems that dominate Libya's climate, effectively suppressing convective activity and deflecting rain-bearing westerly frontal systems further north, away from the Jabal Nafusa Plateau. The specific localized reduction in precipitation observed in Nalut may be an early indicator of this synoptic-scale shift disproportionately impacting the western transitional fringes of the escarpment.

4.2 Socioeconomic Vulnerability and Agronomic Constraints

The empirical manifestation of these hydroclimatic deficits translates directly into profound socioeconomic vulnerabilities for the populations inhabiting Jabal Nafusa. Historically farmed since antiquity, the plateau has relied on the cultivation of resilient tree crops, such as olives, almonds, and figs. However, the data confirm that the fundamental structural imbalance in the water budget, where evaporative demand outpaces supply by factors ranging from 5 to 15, renders rain-fed agriculture severely constrained and structurally fragile. Recent sociological and agricultural surveys in the region highlight that farmers in arable towns such as Yifren, Nalut, Jadu, and Qala'a are increasingly experiencing disrupted harvesting cycles, progressively decreasing yields, and heightened food insecurity directly correlated with changing climate patterns (Wehrey, 2024; Eljadid & MacFee, 2023). The observed warming of winters and intensification of summer desiccation without the historic compensation of predictable seasonal rainfall disrupts the phenological cycles of these essential arboreal crops. Furthermore, because the climatic data confirm the absence of a naturally occurring effective meteorological recharge window, unmanaged extraction for urban or agricultural utilization implicitly relies on the depletion of local, often disconnected, deep fossil groundwater reserves. In areas geographically isolated from the distribution networks of the Man-Made River, the compounding pressures of an accelerating climatic water deficit and unchecked groundwater

pumping create a highly precarious hydrological trajectory that threatens the long-term habitability of these highland communities (Saaed, 2025).

4.3 Methodological Limitations and Uncertainties

While the results of this assessment definitively outline a chronic baseline water shortage, it is scientifically imperative to contextualize these findings within the inherent limitations of this methodology. First, relying on a single global gridded product, even one as highly validated as TerraClimate, introduces unavoidable uncertainties regarding the absolute micro-level precision of precipitation and ET_0. In topographically complex areas, such as the Jabal Nafusa escarpment, highly localized orographic rainfall events or microclimatic temperature depressions may be marginally smoothed by the interpolation algorithms inherent in a 4 km grid.

Second, the absence of an active, dense, and continuous terrestrial meteorological network across northwestern Libya precludes direct in-situ numerical validation (e.g., calculating precise local error metrics against ground truth for the 1994–2023 period). While literature-based validations from analogous Southern Mediterranean basins confirm TerraClimate's general reliability and excellent capacity to capture spatial gradients, localized biases, such as a generalized tendency to slightly underestimate peak extreme precipitation events, cannot be perfectly isolated or corrected via quantile mapping in this specific study area.

Finally, defining aridity by substituting PET with ET_0 represents a necessary, albeit widely accepted, approximation. While ET_0 provides a highly robust, agronomically relevant metric based on the ASCE Penman-Monteith equation, true environmental PET may vary depending on native vegetation cover and complex aerodynamic resistances that are not fully captured by a standardized grass reference model. Despite these recognized limitations, the consistency of the west-to-east spatial gradient across multiple independent indices, combined with the rigorous removal of temporal autocorrelation via the Modified Mann-Kendall test, provides high confidence that the relative spatial patterns and monotonic trends presented herein are both mathematically sound and physically representative of the changing Libyan climate.

5. Conclusion and Strategic Policy Implications

5.1 Synthesis of Baseline Findings

This high-resolution, autocorrelation-corrected climatological analysis of the 1994–2023 normal period provides a highly robust empirical foundation for delineating the Jabal Nafusa region as a continuously and increasingly water-stressed environment. The physical magnitude of the evaporative demand over the available precipitation, escalating up to a 15.1-fold volumetric divergence in the western extremities, fundamentally precludes the existence of any naturally occurring moisture surplus throughout the annual cycle.

The application of the Modified Mann-Kendall trend analysis, utilizing the Hamed and Rao variance correction, revealed a structural and statistically significant worsening of the hydroclimatic deficit. This trajectory is defined by rapidly declining precipitation at the western boundary (Nalut) and a significant increase in atmospheric evaporative demand across the

central plateau (Zintan and Gharyan). The integration of the modified UNEP and De Martonne indices unequivocally confirmed an overarching arid classification for the entire mountain range, characterized by a distinct linear mitigating gradient moving from west to east. These findings categorize the stark current climatic reality, effectively bridge historical geographical gaps, and establish a cross-validated quantitative baseline essential for parameterizing complex future drought modeling (e.g., SPEI) across the hyper-arid fringes of NW Libya.

5.2 Strategic Policy Recommendations

Building on these empirical findings, it is evident that proactive, localized, and technically advanced adaptation strategies are urgently required to mitigate the escalating deficits across northwestern Libya. The following strategic directives are recommended to address the identified hydroclimatic vulnerabilities.

The analytical confirmation of a permanent, 12-month climatic water deficit dictates that reliance on local fossil groundwater is a biologically precarious strategy. Strict regulatory frameworks must be enacted by the relevant water authorities to cap unmetered abstraction rates from local plateau aquifers (African Development Bank Group, 2020). Furthermore, the systematic rehabilitation and modernization of traditional runoff-harvesting infrastructures (such as local *Majen* cistern systems and earthen terracing) must be prioritized. These decentralized, localized systems represent the only viable physical method for capturing highly concentrated, intense, and temporally scarce winter precipitation before it is inevitably lost to evaporation or rapid flash-flood runoff.

Agronomic Adaptation and Irrigation Modernization: The temporal mismatch between peak evaporative demand and the absolute cessation of summer precipitation scientifically invalidates the expansion of any rain-fed summer agriculture. Regional agricultural policies must strategically incentivize a transition away from water-intensive cultivation toward highly drought-resistant and high-yield arboreal cultivars (Saaed, 2025). Specifically, the preservation and expansion of resilient varieties of olive, fig, and almond trees, which possess established physiological adaptations suited to the extreme aridity characterizing municipalities such as Nalut and Zintan, should be actively supported.

Where supplemental irrigation is utilized to maintain agricultural viability, a mandatory transition from traditional surface irrigation to high-efficiency pressurized micro-irrigation frameworks is essential. Crucially, future irrigation scheduling must be fundamentally driven by real-time ET_0 monitoring, rather than static theoretical quotas. By precisely matching water application to crop physiological demand and dynamically accounting for the immense atmospheric vaporization forces defined in this study, evaporative losses can be strictly minimized, thereby extending the functional lifespan of the region's critically endangered groundwater reserves.

References

- Abatzoglou, J. T., Dobrowski, S. Z., Parks, S. A., & Hegewisch, K. C. (2018). TerraClimate, a high-resolution global dataset of monthly climate and climatic water balance from 1958–2015. *Scientific Data, 5*, 170191. https://pmc.ncbi.nlm.nih.gov
- Abubakar, H. B. (2024). Evaluation of high-resolution precipitation datasets CHIRPS, TerraClimate and TAMSAT over the Enkangala Escarpment of South Africa. Research Square. https://doi.org/10.21203/rs.3.rs-4365508/v1
- African Development Bank Group. (2020). *Defining a new approach to water management in Libya*. https://www.afdb.org
- Ageena, I. M. (2013). Trends and patterns in the climate of Libya (1945–2010) [Doctoral dissertation, University of Liverpool]. Liverpool Research Archive (LivRepository). https://livrepository.liverpool.ac.uk/17497/
- Ahmed Elbeltagi, Aman Srivastava, Xinchun Cao, Vinay Kumar Gautam, Bilel Zerouali, Muhammad Rizwan Aslam, Ali Salem, Hojjat Emami & Elsayed Ahmed Elsadek. (2025) Bayesian-optimized machine learning boosts actual evapotranspiration prediction in water-stressed agricultural regions of China. *Scientific Reports* 15:1. Crossref https://www.tandfonline.com
- Ali, A. A., & Hafi, A. (2025). Monitoring rainfall variability to assess drought occurrence using SPI and aridity between 1990 and 2020 in Benghazi and surrounding regions, Libya. Journal of Libyan Geological Society, 17(1), 1–18. DOI: 10.13189/ujar.2023.110625
- Altaeb, M., & Sheira, O. (2024). A survey of Libya's environmental challenges. Luiss Mediterranean Platform. https://mp.luiss.it/archives/a-survey-of-libyas-environmental-challenges/
- Blain, G. C. (2013). The modified Mann-Kendall test: On the performance of three variance correction approaches. Bragantia, 72(4), 416–424. https://doi.org/10.1590/S0006-87052013000400007
- Butler, K. (2015). Mann–Kendall for autocorrelated data. University of Toronto Scarborough, Department of Physical and Environmental Sciences. Retrieved from https://www.utsc.utoronto.ca/~butler/climate-lab/mann-kendall-correlated.pdf
- Carnegie Middle East Program. (2024). Climate change in the Middle East and North Africa: Mitigating vulnerabilities and designing effective policies. Carnegie Endowment for International Peace. https://carnegieendowment.org/research/2024/06/climate-middle-east-north-africa-vulnerability
- Collaud Coen, M., Andrews, E., Poulain, A., Baltensperger, U., Bukowiecki, N., & Fierz-Schmidhauser, R. (2020). Effects of the prewhitening method, the time granularity, and the time segmentation on the Mann–Kendall trend detection and the associated Sen's slope. Atmospheric Measurement Techniques, 13(12), 6945–6971. https://doi.org/10.5194/amt-13-6945-2020
- Crapart, C., Anquetin, S., & Audisio, C. (2026). Global projections of aridity index for mid and long-term future based on CMIP6 scenarios. Hydrology and Earth System Sciences, 30, 163–191. https://doi.org/10.5194/hess-30-163-2026
- Eljadid, A. G. (2007). North Libya between arid climate conditions and rainfall changes. Journal of Basic and Applied Sciences, 17(1).

- Eljadid, A., & MacFee, E. (2023). Country report on migration, environment, and climate change in Libya. International Organization for Migration (IOM). https://environmentalmigration.iom.int/sites/g/files/sc5031/f/2023-06-Country_Report_LIBYA.pdf
- Hu, Z., Zhang, Q., Li, J., & Chen, X. (2020). Modified Mann-Kendall trend test for hydrological time series under the scaling hypothesis and its application. Hydrological Sciences Journal, 65(14), 2419–2433. https://doi.org/10.1080/02626667.2020.1810253
- International Organization for Migration. (2025). Libya – Climate change, food security, and migration report. Displacement Tracking Matrix (DTM). International Organization for Migration. https://reliefweb.int/report/libya/displacement-tracking-matrix-dtm-libyas-migrant-report-round-58-may-july-2025
- Kessabi, R., Hanchane, M., Krakauer, N. Y., Kharroubi, A., Mohammed, A., & Elbououchay, M. (2023). Performance evaluation of TerraClimate monthly rainfall data after bias correction in the Fes-Meknes region (Morocco). Climate, 11(6), 120. https://doi.org/10.3390/cli11060120
- Martínez Cortina, L. (Ed.). (2002). Groundwater intensive use: Selected papers. International Conference on Groundwater Intensive Use, València, Spain. SINEX. https://hdl.handle.net/123456789/60038
- Ouassanouan, Y., Simonneaux, V., Kharrou, M. H., Fakir, Y., Baba, M. W., Hssaine, B. A., Hachimi, C. E., Sourp, L., & Chehbouni, A. (2025). Downscaled ERA5 Land addresses agrometeorological data scarcity in North African basins. *Scientific reports*, *15*(1), 38533. https://doi.org/10.1038/s41598-025-20552-2
- Patakamuri, S. K. (2025). modifiedmk: Modified versions of Mann-Kendall and Spearman's rho trend tests (R package, Version 1.6) [Computer software]. CRAN. https://cran.r-project.org/package=modifiedmk
- Saaed, M. W. B. (2025). Understanding the challenges in Libyan rangeland conservation: Exploring pathways to sustainable rehabilitation. In G. Gintzburger & S. Saïdi (Eds.), The rangelands of Libya. CABI. https://www.cabidigitallibrary.org/doi/book/10.1079/9781800627154.0000
- Shazil, M. S., Aleem, M., Ahmad, S., Abdullah, A., & Greco, R. (2025). Assessing the Accuracy of Gridded Precipitation Products in the Campania Region, Italy. *Water*, *17*(17), 2585. https://doi.org/10.3390/w17172585
- Ssembajwe, R., Ngatia, J., et al. (2025). Evaluation of gridded and reanalysis vapour pressure deficit datasets over East Africa. Journal of Southern Hemisphere Earth Systems Science, 75(3), 25004. https://doi.org/10.1071/ES25004
- Taïbi, S., Zeroual, A., & Meddi, M. (2022). Effect of autocorrelation on temporal trends in air-temperature in northern Algeria and links with teleconnections patterns. Theoretical and Applied Climatology, 150(1–2), 517–528. https://doi.org/10.1007/s00704-022-04242-0
- Tegos, A., Stefanidis, S., Cody, J., & Koutsoyiannis, D. (2023). On the sensitivity of standardized-precipitation-evapotranspiration and aridity indexes using alternative potential evapotranspiration models. Hydrology, 10(3), 64. https://doi.org/10.3390/hydrology10030064
- United Nations Educational, Scientific and Cultural Organization (UNESCO). (1999). Proceedings of the International Conference on Regional Aquifer Systems in Arid Zones: Managing non-renewable resources, Tripoli, Libya, 20–24 November 1999. Technical Documents in Hydrology, No. 42. Paris, France: UNESCO. https://unesdoc.unesco.org/ark:/48223/pf0000127080

- Wehrey, F. (2024). Climate vulnerability in Libya: Building resilience through local empowerment. Carnegie Endowment for International Peace. https://carnegieendowment.org/research/2024/06/libya-climate-vulnerability-adaptation-periphery
- Xiang, K., Li, Y., Horton, R., & Feng, H. (2020). Similarity and difference of potential evapotranspiration and reference crop evapotranspiration – a review. Agricultural Water Management, 232, 106043. https://doi.org/10.1016/j.agwat.2020.106043
- Zomer, R. J., Trabucco, A., & Coen, G. (2022). Version 3 of the Global Aridity Index and Potential Evapotranspiration Climate Database. Scientific Data, 9(1), 117. https://doi.org/10.1038/s41597-022-01230-1
- Zomer, R. J., Xu, J., Simonetti, D., & Runge, J. (2025). CMIP6-based global estimates of future aridity index and potential evapotranspiration for 2021–2060. Open Research Europe, 4, 157. https://doi.org/10.57760/sciencedb.nbsdc.00086